Low temperature growth of pyroelectric triglycine sulfate single crystal for passive infrared sensing

Cite as: AIP Conference Proceedings **2115**, 030400 (2019); https://doi.org/10.1063/1.5113239
Published Online: 12 July 2019

Surender P. Gaur, Sandhya, Sushil Kumar, Sk Riyajuddin, Sunny Kumar, Damini Badhwar, and Kaushik Ghosh

Low temperature growth of pyroelectric triglycine sulfate single crystal for passive infrared sensing

Surender P. Gaur[1, a], Sandhya[2], Sushil Kumar[1], Sk Riyajuddin[1], Sunny Kumar[1], Damini Badhwar[1], Kaushik Ghosh[1]

[1] *Institute of Nano Science and Technology (INST), Mohali, India-160062*
[2] *Department of Electronic Science, Kurukshetra University, Kurukshetra, India-136119*

[a] *Corresponding author:* surender.rp431741@inst.ac.in

Abstract. Synthesis, characterization and pyroelectric investigations on low temperature grown triglycine sulfate (TGS) single crystal is reported. Low temperature growth in this work was adopted to examine the effects on dielectric properties and pyroelectric responsivity. Developed crystal was found highly transparent on wavelengths from 223 nm to 1100 nm and free energy band was calculated to be 5.5 eV. The lattice structure of crystal was confirmed monoclinic with space group $P2_1$. Dielectric permittivity ($\mathcal{E}$) of the crystal measured at 27 ºC was found 20. The pyroelectric current (I_P) perceived in the study yield pyroelectric coefficient (ρ) of 3.34×10^{-8} C/cm^{2}K and consequently the $\rho/\mathcal{E}$ figure of merit (*Fv)* to be 0.166×10^{-8} C/cm^{2}K. An additive enhancement in the pyroelectric figure of merit (*Fv)* was calculated due to the lower value of dielectric permittivity.
Keywords: triglycine sulfate, pyroelectric coefficient, infrared detector**,** dielectric permittivity.

1. INTRODUCTION

Pyroelectric detector is the most accepted form of the uncooled infrared detectors due to their faster response, bias free operation and simple architecture [1]. Single crystal triglycine sulfate (TGS), chemical formula $(NH_2CH_2COOH)_3\ H_2SO_4$ is preferred ferroelectric material used for high detectivity indoor infrared detection. The crystal gains its popularity due to the ideal pyroelectric properties i.e. large pyroelectric coefficient, moderate dielectric constant and wide band spectral response [2-4]. The crystal exhibits spontaneous polarization along <010> axis in ferroelectric phase but the polarization disappears as the crystal changes its phase from ferroelectric to paraelectric. As the crystal has low phase transition or Curie temperature (T_C =49 ^oC) the use of the crystal is restricted with ferial temperature applications only [4].

Basic lattice structure of the TGS crystal is monoclinic with space group $P2_1$ in ferroelectric phase ($T < T_C$), in second order or paraelectric phase ($T > T_C$), the space group gets transform from $P2_1$ to $P2_{1/m}$ by introducing two mirror planes along Y- axis, at Y=0.25 and Y=0.75. A significant increment in phase transition temperature up to 57 °C has been accomplished by deuterization [5]. Doping of amino acid L-alanine in little percentage can make the crystal to retain the ferroelectric properties of crystal after a few extent of Curie temperature [6]. Moreover this the doping of crystal with cations like Cd, Mn and Zn etc. is also used to enhance the Curie temperature effectively [7-8]. Essentially the TGS crystal loses its spontaneous polarization above Curie temperature. But the ferroelectric decomposition of the crystal initiates at 80 °C and gets permanently decomposed above 115 °C [9]. Though, Curie temperature of the crystal can be improved to some instance by above listed methods but the crystal is still preferred in its pure form for low temperature applications.

In this work the single crystal of triglycine sulfate was developed at relatively lower temperature to study its effect on dielectric properties and pyroelectric responsivity. The chemical, structural and thermoelectric characterizations of the crystal were made with appropriate methods. Free energy band (*Eg*) and optical non

DAE Solid State Physics Symposium 2018
AIP Conf. Proc. 2115, 030400-1–030400-4; https://doi.org/10.1063/1.5113239
Published by AIP Publishing. 978-0-7354-1851-6/$30.00

linearity were evaluated through UV-Visible spectroscopy. Crystal lattice structure and dielectric properties were examined using XRD and LCR network analyzer. The pyroelectric response and phase transition temperature of the crystal were deliberated on a dynamic heating setup of adjustable heater frequency

2. MATERIAL AND METHODS

TGS single crystal was developed at relatively lower temperature of 16 ± 0.8 °C in controlled ambient through solvent evaporation method. Basic solution was prepared by using analar grade glycine powder (NH_2CH_2COOH), concentrated sulfuric acid (H_2SO_4) and DI water of resistivity 18 MΩ as solvent. The glycine powder and sulfuric acid in molar concentration of 3:1 were mixed in 20 ml of water [10-13]. Mixture was stirred for two hours at 40 °C at 350 rpm. A clear solution of pH value 3.5 was generated for crystal growth. Temperature of growth ambient was maintained at 16 ± 0.8 °C. Seed crystal was observed at the bottom of the container after four days. It took sixteen days in developing single crystal of triglycine sulfate of dimensions 10 mm × 8 mm × 6 mm.

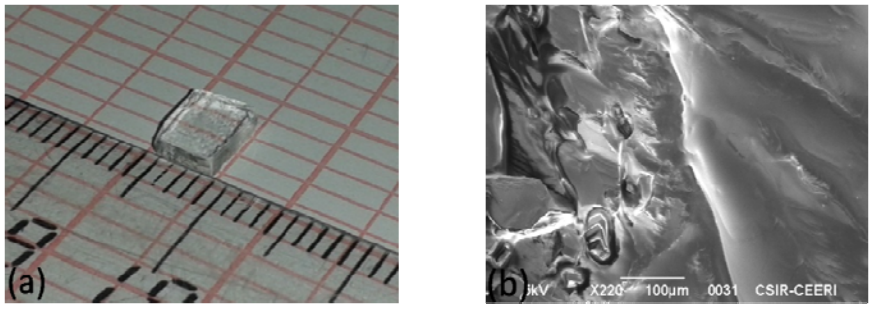

FIGURE 1 (a) Low temperature grown TGS crystal, **(b)** SEM micrograph presenting the (010) plane topology of grown TGS crystal

3. CHARACTERIZATION AND DISCUSSION

The elemental composition of the developed crystal is examined by using energy dispersive X-ray spectroscopy (JEOL-JSM639OLV). Detailed atomic and weight percentage of all elements present in the crystal is given in table1. Due to very low energy the presence of hydrogen atoms in the crystal is not sensed by EDX system. The optical image and SEM surface profile of the crystal at 5 kV are shown in figs 1 (a) and (b).

TABLE 1 atomic and weight percentage of elements in TGS

Element	Atomic (%)	Weight (%)
C	23.35	28.88
N	13.59	14.41
O	59.12	54.89
S	03.94	01.82
Total	100.00	100.00

UV- Visible spectroscopy on liquid sample is carried out on wavelengths from 200-1100 nm, covering partial ultraviolet, entire visible and near infrared region of electromagnetic spectrum. The cut off wavelength of UV transmittance at 222 nm is recorded. Crystal offers a uniform transmittance of 90-95 % on wavelengths 240 - 1000 nm. As the crystal offer a low cut off wavelength and good optical transmittance the study validates the non linear optical characteristics of crystal and its suitability for optoelectronic applications [14]. The free energy band of the crystal is calculated by equation (1).

$$Ev\,(j) = {}^{hc}/_{\lambda} \tag{1}$$

where h = Plank`s constant, c = velocity of light and λ = wavelength of transmittance. In present case the free energy band at 222 nm is found to be 5.5 eV which is in good agreement with available reports [15, 16].

X-ray diffraction (XRD) analysis was employed to classify the structural parameters of crystal. Study was performed on Phillips X'pert PRO, X-ray diffractometer with Cu-Kα radiation (λ= 1.54178 Å) over 10°-45° [7]. The spectral intensity distribution graph of pure TGS powder is shown in fig 2 (b). From study it is concluded that the crystal has monoclinic lattice structure of space group $P2_1$. The lattice parameters calculated by analysis are a = 9.161, b = 12.586, c = 5.718 and β = 105.49.

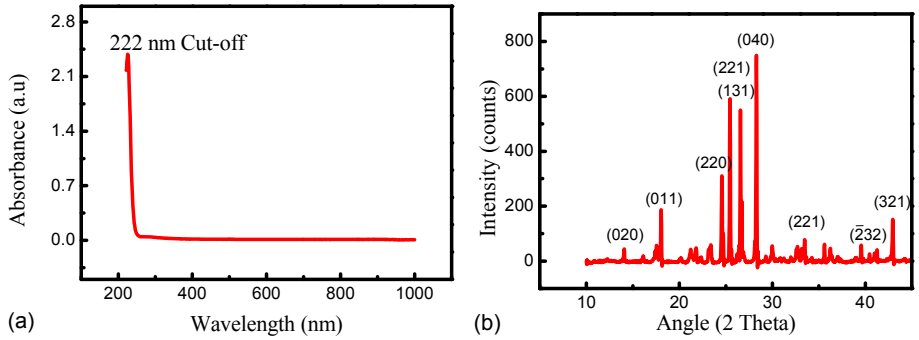

FIGURE 2 (a) Optical absorbance spectra (λ=200-1100 nm) of UV-Vis. spectroscopy for developed TGS crystal, **(b)** X-ray Dispersive graph of powdered sample of TGS crystal

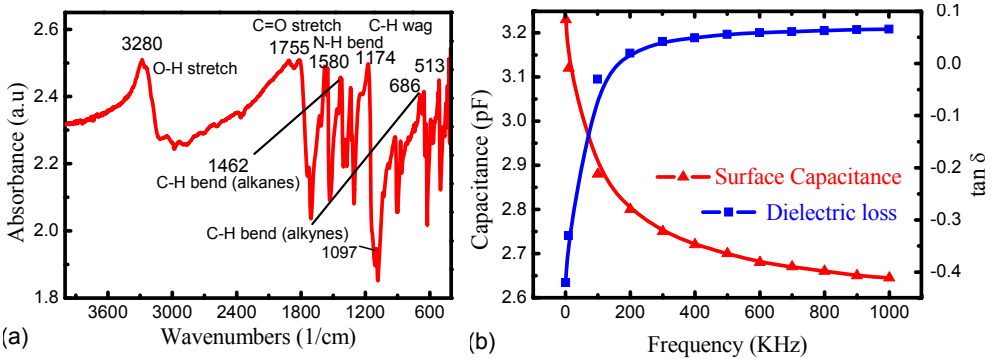

FIGURE 3 (a) FTIR spectra of developed TGS crystal, **(b)** Frequency vs. Surface capacitance and dielectric losses

Powdered sample of triglycine sulfate was examined by IR absorption over the wave numbers 4000 cm^{-1} to 400 cm^{-1} to identify the functional groups and bond structure of the molecules. System generated absorption graph is verified with the existing FTIR data analysis from literature. Infrared absorption peaks obtained at wave number 513 cm^{-1} and below characterize the NH_3^+ cycles in the sample. Absorption region extended between 2750 cm^{-1} and 2050 $cm^{-1}$is in response of stretching mode of hydrogen bonded NH_3^+ combination bands. Significant absorption recorded at 1097 cm^{-1} includes the sulfate content in the sample. Similarly absorption peaks obtained at 686 cm^{-1} and 1462 cm^{-1} verifying the C-H bend of alkynes and alkenes group. Absorption peak at 1174 cm^{-1} signify the C-H wag (-CH_2 COOH) of alkyl halides. Infrared absorption at 1755 cm^{-1} is assigned to C=O stretching of –COOH group. Broad absorption band from 3500 cm^{-1} 3200 cm^{-1} indicates the O-H stretch of carboxyl group in the crystal molecule.

Dielectric properties of the crystal were examined on Agilent 4284A LCR measurement setup. Electrical contacts were developed on (010) and ($0\bar{1}0$) facets by low vacuum DC sputtering of Au. Fixed bias analysis was made with an applied signal voltage of 100 mV. Signal frequency was adjusted from 1.0 KHz to 1.0 MHz. Graphs obtained between signal frequency and surface capacitance is shown in fig 3 (b). A steady variation in dielectric losses from 0.001 to 0.065 is recorded over different applied frequencies from 1.0 KHz to 1.0 MHz. The dielectric

losses recorded in study are within acceptable limit and identical with the same in [12]. The dielectric constant (Ɛ) calculated for the crystal at given temperature is found to be 20 at 27 °C, dielectric constant calculated for low temperature grown crystal is measured lower than higher temperature growth [11].

Pyroelectric response of the crystal measured at the planes perpendicular to the polar axis. i.e. along Y-axis. Electrical contacts are made at (010) and $(0\bar{1}0)$ planes by low temperature DC sputtering of Au. A dynamic heating setup of adjustable heater frequency was used for the thermal excitations of the crystal. The heater frequency was adjusted at 1.0 Hz and a net temperature variation of 0.2 °C was maintained in the experiment. The measurements are carried out at ambient temperature of 27 °C. Equation (2) is used to calculate the pyroelectric coefficient of the crystal.

$$\rho = \frac{Ip}{2\pi.f.A_d.\Delta T} \tag{2}$$

where *Ip* =pyroelectric current, ρ= pyroelectric coefficient, *f*= frequency of thermal excitation, *Ad*= surface area of the detector (crystal) and ΔT=change in temperature.

The pyroelectric figure of merit (F_V) and figure of detectivity (F_D) used to determine the suitability of a material in development of pyroelectric detector was calculated by using equation (3) and (4).

$$F_V = \frac{\rho}{\varepsilon} \tag{3}$$

$$F_D = \frac{\rho}{c_p\sqrt{\varepsilon.\tan\delta}} \tag{4}$$

Where c_p = volume heat capacity, $\mathcal{E}$= dielectric constant of detector material and tan δ is dielectric loss

The pyroelectric coefficient and pyroelectric figure of merit calculated for the crystal by using (2) and (3) are 3.34×10^{-8} C/cm^{2}K and 0.166×10^{-8} C/cm^{2}K respectively. The figure of detectivity (F_D) calculated by (4) was 5.5×10^{-5} Pa$^{-1/2}$.

4. CONCLUSION

Single crystal of triglycine sulfate was developed at relatively low temperature to study its effects on dielectric and pyroelectric properties. The developed crystal is characterized using EDX, UV-Visible spectroscopy, FTIR, XRD and network analyzer methods. The crystal exhibits relatively low dielectric constant (ε) of 20 at 27 ºC. The grown single crystal of pure TGS offer an intended free energy band (*Eg*) of 5.5 eV. Lattice structure was confirmed as monoclinic of space group $P2_1$. The pyroelectric current (I_P) measured has perceived pyroelectric coefficient (ρ) of 3.34×10^{-8} C/cm^{2}K at 27 ºC and consequent $\rho/\mathcal{E}$ figure of merit (F_v) to be 0.166×10^{-8} C/cm^{2}K.

REFERENCES

1. G. Hyseni, N. Caka, H. Kujtim, W. seas Transactions on Circuits and Systems, 4(9), 238-247, (2010).
2. R.B. Lal and A.K. Batra, Ferroelectrics, 142(1), (1993).
3. P.J. Lock, Appl. Phys. Letters, 19, 390, (1971).
4. M.D. Aggarwal, A.K. Batra, P. Guggilla, and M.E. Edwards, NASA/TM–216373, (2010).
5. A. K. Batra, M. D. Aggarwal and R. B. Lal, Materials Letters, 57, 3943-48, (2003).
6. P. R. Deepthi, and J. Shanthi, International Journal of Engineering Research & Technology, 3 (6), (2014).
7. F. Khanum and J. Podder, International Journal of Optics, 803797, (2012).
8. S. Balakumar and H.C. Zeng, Journal of materials chemistry, 10, 651-656, (2000).
9. H. Schmidt and V. Ziebert, Ferroelectrics, 6, 151, (1974).
10. R. Renugadevi, G. Kanchana and R. Kesavasamy, Elixir Crystal Growth, 55A, 13033-13035, (2013).
11. P.H. Beerman, Infrared Physics, 15, 225-131, (1975).
12. S. Suresh, A. Ramanand, D. Jayaramana, P. Manib, Optoelectronics and advanced materials, 4(11), 1763 – 1765, (2010).
13. M. S. Pandian, N. Balamurugan, V. Ganesh, P.V.R. Shekar, K.K. Rao, P. Ramasamy, Materials Letters, 62, 3830–3832, (2008).
14. F. Khanum and J. Podder, Journal of Crystallization Process and Technology, 1, 49-54, (2011).
15. M.S. Pandian, P. Ramasamy, B. Kumarm, Materials Research Bulletin, 5557, (2012,)
16. L.E. Garen and E.J. Sharp, IEEE Transactions on Parts, Hybrids and packaging, 10(4), (1974).